International Journal of Innovative Technology and Exploring Engineering (IJITEE)
ISSN: 2278-3075 (Online), Volume-8 Issue-10, August 2019

Optimal Fractional Order PID Controller for Centralized and Decentralized Frequency Control in Restructured Power System

S. Jennathu Beevi, R. Jayashree

***Abstract*: In this research paper, an attempt has been made to design a Fractional order PID (FOPID) controller employed for centralized and decentralized frequency control in a restructured power system. The controller gains are optimized by Moth Flame Optimization algorithm (MFO), with Integral Time Absolute Error (ITAE) as objective function. The performance of the FOPID controller is compared with that of conventional PID controller under various contract scenarios. It is observed that FOPID as a frequency error damping controller, the steady state and dynamic performance of the proposed power system is enhanced.**

***Index Terms*: Automatic Generation Control, Bilateral Contracts, Fractional Order Controller, Regulation.**

I. INTRODUCTION

Power system control is one of the most critical and essential functions in a power market as both active and reactive power requirements are never constant and are increasing or decreasing continuously. The deviations in the frequency must be eliminated by balancing active power generation with the load through a proper control mechanism. In restructured power structure, the centralized frequency correction service is termed as Regulation or Automatic Generation Control (AGC) and the decentralized frequency regulatory service is known as Load Following (LF). Among the various control strategies, AGC [1] is the basic control structure in the power system operation. The various problems of load frequency control after deregulation have been reviewed in detail [2-6]. The major approaches used for frequency control which focus on designing proportional-integral-derivative (PID) controller [7], contemporary control approaches [8-12]. Intelligent control schemes such as neural networks [13-14] fuzzy logic-based control [15] and Soft computing-based approaches for controller parameter tuning are found in the literature. In most of the literature, PID controller has been used for eliminating the frequency error. Over the past few years, a increasing interest has been shown in fractional order controller, which has inspired many issues in the fields of automation, robotics, energy systems, etc. to be solved efficiently. The authors in [16-17] have applied fractional-order proportional–integral–derivative controller (FOPID) for automatic generation control (AGC). The authors in [18] have analyzed “deregulated AGC Multi area system using FOPI and FOPID cascaded controller with geothermal, solar and thermal power plants". Rajesh [19] has applied load following controller for AGC in restructured power system. For frequency regulation in conventional power system as well as restructured power system, mostly the traditional PID controller has been used. Even though, the PID controller exhibits good dynamic performance characteristics, alternate controllers like FOPID are applied for frequency control in conventional vertically integrated utilities and restructured power structure as well. Also, PID controller has only three gains *Kp*, *Ki* and *Kd* as tuning parameters, whereas FOPID controller has five tuning parameters, *Kp*, *Ki*, *Kd*, λ and μ. The additional two degree of freedom makes the FOPID more adaptable and robust.

According to the optimization theorem of No-Free-Lunch (NFL) [20], not all algorithms can solve all the issues of optimization. Fractional order systems are based on fractional order calculus [21-22] which, with few coefficients, can represent dynamic systems with high order dynamics and complicated nonlinear phenomena. The dynamics of the integer-order portray the particular and lower class of fractional-order systems.Thus, as established by many researchers, such as [23-24], fractional-order controllers surpassed their counterparts in the integer-order. The author in [25], proposed MFO, a nature inspired optimization algorithm. In recent years, MFO algorithm has been found effective for many of the power system optimization problems [27-30]. Even though there are many population-based algorithms available for optimization, MFO has been chosen in our present work because of its simplicity does not need any information about the system, (i.e.) the mathematical background of the proposed system. Being a population-based algorithm, local optima is avoided which makes it suitable for practical applications. MFO can also handle constrained and unconstrained problems. MFO depends much on problem representation than the nature and structure of the problem. Therefore, it can be readily used for any type of optimization problem. It is observed in the literature that, MFO is highly efficient in achieving the global optimum, and is also efficient in balancing search space exploration and exploitation.

Manuscript published on 30 August 2019.
*Correspondence Author(s)
S. Jennathu Beevi, Department of EEE, B. S. AbdurRahman Crescent Institute of Science and Technology, Vandalur, Chennai, (Tamilnadu), India. E-mail: jennathb@gmail.com
R. Jayashree, Department of EEE, B. S. AbdurRahman Crescent Institute of Science and Technology, Vandalur, Chennai, (Tamilnadu), India.

Due to the adaptive convergence characteristic, MFO has very good convergence speed. Hence in our present work MFO is selected as an optimizer for minimizing the frequency error. In the literature, the performance index Integral Time Absolute Error(ITAE) is widely used for optimization. ITAE criteria gives integration of time multiplied by Absolute Error and weightage is given to those which exist over a longer time than those at the initial stage. The reduction in settling time is achieved by allocating larger multiplication factor to the error at final stages rather than the initial ones. The objectives of the present article are:(i)To Simulate the centralized and decentralized control strategy in a two-area restructured power system using PID and FOPID controller with bilateral contract structure under for different cases.(ii) To obtain the optimal controller gains using MFO algorithm by employing ITAE as objective function. And (iii) To prove the effectiveness of FOPID controller over PID via qualitative and quantitative analysis of results. To prove the effectiveness of the FOPID controller and MFO algorithm, the system given in [19] is taken for simulation.

II. SYSTEM UNDER STUDY

A. Components of the proposed system

In the proposed system [19], there are two control areas in which each area has two GCs and two DCs respectively. Both the GCs are having non-reheat thermal units and the DCs which have the liberty of any GC to contract. Any DC in region1 may contract separately through bilateral transactions with any GC in another control region, say Area-2. The Disco Participation Matrix (DPM) shows the different Contract Participation Factors (fcp) agreements that occur between GCs and DCs.

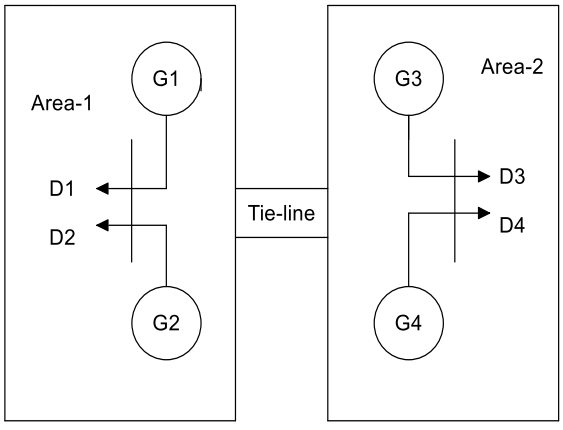

Fig. 1 Structure of two- area interconnected power system in competitive market

The diagonal blocks of the DPM given by equation.4 corresponds to local demands i.e the demands of DCs in an area from the GCs in the same area. The demand of the DCs in one area from the GCs in another area is represented by the off-diagonal blocks.

Fig.1 illustrates the competitive two area power system. The two-area interconnected system transfer function model is shown in Fig.2.The notations used in the block diagram are explained in Appendix I.As shown in Fig.2, in the two-area interconnected system, the governor, turbine and the power system are represented by their equivalent transfer function models. In each area there is an AGC controller to distribute the ACE errors to the areas.

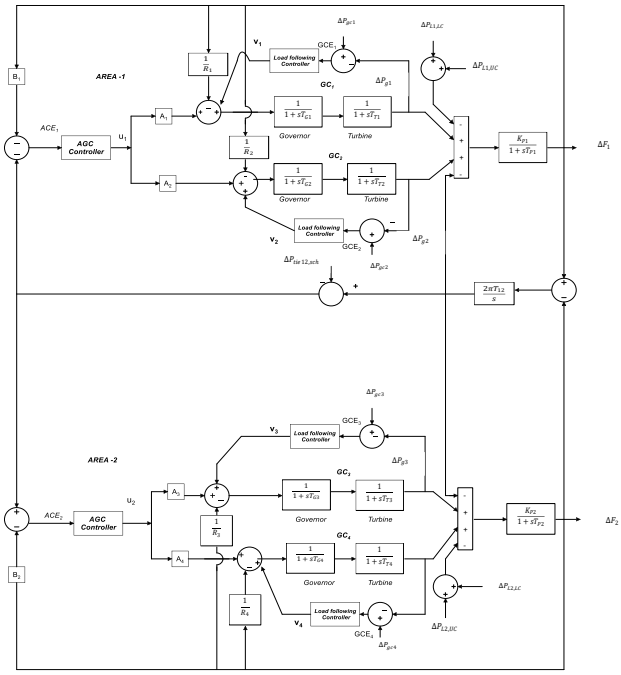

Fig. 2 Decentralized and Centralized frequency control scheme for two area restructured power system[19]

This functions as a primary control mechanism to bring to zero the deviations in frequency and tie line power.Each generating unit is supported by a load following controller locally which helps the generation units to supply the power contracted by the loads.The ACE signal is given as input to the AGC controller.For the load following controller,Generation Control Error (GCE) is given as input signal.Parameters of the framework used for simulation are given in Appendix. II.

The heat units used in each region have a 10 percent GRC (Generation Rate Constraint), as shown in Figure 3.

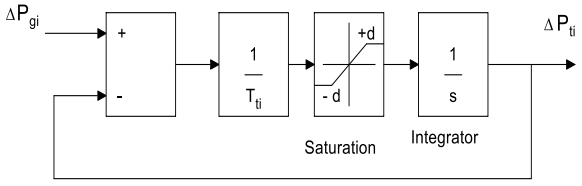

Fig. 3 Generation Rate Constraint

Bilateral contract between a GC and a DC can be related by DC participation Matrix known as DPM. Asthe proposed system has NG =4 and ND =4, the DPM will be of the order of 4 x 4.

Retrieval Number: I8711078919/19©BEIESP
DOI: 10.35940/ijitee.I8711.0881019
Journal Website: www.ijitee.org

Published By:
Blue Eyes Intelligence Engineering and Sciences Publication (BEIESP)

$$DPM = \begin{bmatrix} fcp_{11} & fcp_{12} & fcp_{13} & fcp_{14} \\ fcp_{21} & fcp_{22} & fcp_{23} & fcp_{24} \\ fcp_{31} & fcp_{32} & fcp_{33} & fcp_{34} \\ fcp_{41} & fcp_{42} & fcp_{43} & fcp_{44} \end{bmatrix} \quad (1)$$

The GCs and DCs are represented by the rows and column of the DPM matrix respectively. The fcp is the ratio of the power demanded from m^{th} GC to the total demand of n^{th}DC. In this matrix, the sum of all the entries in a column is unity.The contracted power of GCs with DCs is given by

$$\Delta P_{gcm} = \sum_{n=1}^{NDC} cpf_{mn} \Delta P_{Ln} \quad (2)$$

where ΔP_{gcm} is the contracted power of m^{th}generating unit, ΔP_{Ln} total demand of n^{th}DC and fcp_{mn} contract participation factor between n^{th}DC and m^{th}GC. The scheduled steady state power flow on the tie-line is given as,

$\Delta P_{tie12,\,sch}$= *(Demand of DCs in area-2 from GCs in area-1) – (Demand of DCs in area-1 from GCs in area-2)* (3)

The scheduled power flow on the tie-line at steady state is calculated as,

$$\Delta P_{tie12,sch} = \sum_{m=1}^{2} \sum_{n=3}^{4} cpf_{mn} \Delta P_{Ln} - \sum_{m=3}^{4} \sum_{n=1}^{2} cpf_{mn} \Delta P_{Ln} \quad (4)$$

The tie-line power error, $\Delta P_{\,tie12,\,err}$ is the difference between the actual power flow and the scheduled power flow.

The actual tie-line power flow is equal to the scheduled power flow at steady state. Hence, tie-line power error, $\Delta P_{tie12,err}$ reduces to zero. The ACE signals are generated using this error signal.

$$ACE_i = B_i \Delta F_i + \Delta P_{tie12,err} \quad (5)$$

The contracted power of DCs are illustrated in Fig.4

In each area two types control actions take place. The first one is Frequency Regulation or AGC which is the centralized control. AGC controller is fed with ACE as input signal. The other one is Load Following (LF) action which is a decentralized control. As seen from the above figure, the contracted load signal ΔP_{gcn} originates from a n^{th} DC is compared with the generated output signal of m^{th} GC, ΔP_{gm}. This is applicable while m^{th} GC and n^{th} DC are in contract. The difference between ΔP_{gcn} and ΔP_{gm} is known as Generation Control Error (GCE). This is given as input command signal to the LF units. The LF controller reduces GCE by following the load. By minimizing this error, the generating units are made to supply the contracted power to the loads.

GCE for the load following units are given by Eqn. (6)

$$GCE_m = \Delta P_{gcn} - \Delta P_{gm} \quad (6)$$

$\Delta P_{L1,\,LC}$ is the sum of contracted power demanded by DC_1 and DC_2. Similarly, $\Delta P_{L2,\,LC}$ is the sum of contracted power demanded by DC_3 and DC_4. The noncontracted demands of DCs areΔP_{UC1}, ΔP_{UC2}, ΔP_{UC3} and ΔP_{UC4}. The distribution of noncontracted power is resolved by the ACE Participation Factors (fcp) among various GCs in each area at steady state. It is important to note that the apfs, A_1+A_2 = 1.0 in Area -1 and A_3+A_4 = 1.0 in Area-2.

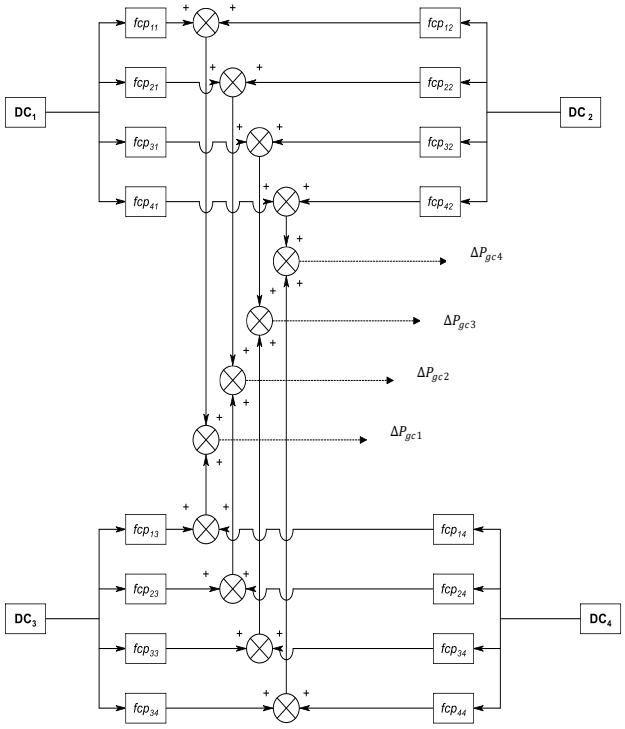

Fig. 4 Contracted power of DCs in competitive ancillary service market

B. Case Description

The three different cases simulated along with bilateral contracts are explained in Table.1.

Table 1: Description of control scenarios

Case No	AGC		Load following				Contract Violation
	Area 1	Area 2	GC 1	GC 2	GC 3	GC 4	
Case 1	No	No	No	Yes	No	Yes	No
Case 2	Yes	Yes	No	Yes	No	Yes	No
Case 3	Yes	Yes	No	Yes	No	Yes	Yes

Case 1: Only load following, No contract violation

It is assumed that no GC participates in AGC and there is no contract violation. In Area-1, GC1 is for speed regulation and GC2 is for load following. Also, in Area-2, GC3 is for speed regulation and GC4 is for load following. Since there is no AGC, no centralized controller is available.

Published By:
Blue Eyes Intelligence Engineering
and Sciences Publication (BEIESP)

All the DCs are assumed to have a load of 0.005 puMW each. The contracts between the GCs and DCs in both the areas are described in DPM given in Eqn. (7).

$$DPM = \begin{bmatrix} 0 & 0 & 0 & 0 \\ 0.25 & 0.10 & 0.75 & 0.60 \\ 0 & 0 & 0 & 0 \\ 0.75 & 0.90 & 0.25 & 0.40 \end{bmatrix} \quad (7)$$

Also, it is assumed that there is no contract violation. It is assumed that all the four DCs possess a load demand of 0.005 puMW which is contracted to the available GCs as per the DPM given above. Hence $\Delta P_{L1}=\Delta P_{L2}= \Delta P_{L3}=\Delta P_{L4}$ =0.005puMW. Therefore, the contracted local load for Area-1 is 0.01pu MW and for Area-2 is 0.01pu MW. At steady state the generating unit generates power equal to the power contracted by the respective unit given by,

$$\Delta P_{gm,s} = \Delta P_{gcm} \quad (8)$$

It is calculated for each GC using the DPM given above using equations (2) and (8) and given in Table.2. The steady state outputs of the Gencos in Area 1 & 2 are calculated using the DPM given in Eqn. (7). The tie-line power scheduled is calculated using Eqn. (4) is -0.0015 p.uMW.

Case 2: Both AGC and load following

Table 2 illustrates the distribution of contracted power from the Gencos to the respective Discos. The GC_1 and GC_3 are under AGC. The DPM is same as in Case 1.The ACE participation factors for the GC_1 and GC_3 are 1. GC_2 and GC_4 are under LF. Therefore, ACE participation factors for GC 2 and GC 4 are zero. It is also assumed that there is no non contracted demand in any of the areas. The DCs have 0.005 puMW of contracted demand which is to be met by the GC_2 and GC_4 since these two participate in load following. The GCs outputs at steady state are same as Case 1.The steady state generated outputs of the four Gencos are same as in Case 1, and the values are given in Table 3. The tie-line power scheduled is calculated using Eqn. (5) is -0.0015 p.uMW, same as in Case 1 since there is no contract violation.

Table 2: Steady state output of Gencos – Case 1 and Case 2

Genco	Steady State output in puMW
$\Delta P_{g1,ss}$	(0+0+0+0) x0.005 = 0
$\Delta P_{g2,ss}$	(0.25 +0.1+ 0.75 + 0.60) x 0.005 = 0.0085
$\Delta P_{g3,ss}$	(0 + 0 + 0 + 0) x 0.005 = 0
$\Delta P_{g4,ss}$	(0.75 + 0.9 + 0.25 + 0.4) x 0.005 = 0.0115

Case 3: Both AGC and load following with contract violation

In this case, an uncontracted load demand of 0.005 puMW is introduced in Area-1.The contracted demand, DPM and APFs are same as in Case 2. This uncontracted demand along with the contracted demand of 0.005 puMW will introduce error in Area-1 ACE. This can be nullified by additional generation by the GCs in Area-1. As there are two GCs in Area-1, this uncontracted demand will be shared among the two GCs. The amount of sharing depends on the value of APFs. In the presence of uncontracted demand, the steady state power output of the GCs gets modified according to Eqn. (9).

$$\begin{bmatrix} \Delta P_{g1,ss} \\ \Delta P_{g2,ss} \\ \Delta P_{g3,ss} \\ \Delta P_{g4,ss} \end{bmatrix} = \begin{bmatrix} A_1 & 0.0 & 0.0 & 0.0 \\ 0.0 & A_2 & 0.0 & 0.0 \\ 0.0 & 0.0 & A_3 & 0.0 \\ 0.0 & 0.0 & 0.0 & A_4 \end{bmatrix} \begin{bmatrix} \Delta P_{L1,UC} \\ \Delta P_{L2,UC} \\ \Delta P_{L3,UC} \\ \Delta P_{L4,UC} \end{bmatrix} + \begin{bmatrix} \Delta P_{gc1} \\ \Delta P_{gc2} \\ \Delta P_{gc3} \\ \Delta P_{gc4} \end{bmatrix} \quad (9)$$

The GC_1 sharing of apf is 1 i.e, $A_1 = 1$ and of GC_2 i.e $A_2 = 0$. Hence the additional generation will be favored by GC_1 in Area-1.

Table 3: GENCOs output power as per Disco demands for Case 1 and Case 2

		Area-1		Area-2		Total (puMW)
		DC_1	DC_2	DC_3	DC_4	
Case 1	GC_1	0	0	0	0	0
	GC_2	0.00125	0.0005	0.00375	0.003	0.0085
	GC_3	0	0	0	0	0
	GC_4	0.00375	0.0045	0.00125	0.002	0.0115
Case 2	GC_1	0	0	0	0	0
	GC_2	0.00125	0.0005	0.00375	0.003	0.0085
	GC_3	0	0	0	0	0
	GC_4	0.00375	0.0045	0.00125	0.002	0.0115

Table 4: Steady state output of Gencos – Case 3

Genco	Components of Contract violation	Steady State output in puMW
$\Delta P_{g1,ss}$	$(A_1 \times \Delta P_{L1,UC}) + \Delta P_{gc1}$	(1 x 0.005) +0= 0.005
$\Delta P_{g2,ss}$	$(A_2 \times \Delta P_{L2,UC}) + \Delta P_{gc2}$	(0 x 0.005) +0.0085= 0.0085
$\Delta P_{g3,ss}$	$(A_3 \times \Delta P_{L3,UC}) + \Delta P_{gc3}$	(1 x 0) +0 = 0
$\Delta P_{g4,ss}$	$(A_4 \times \Delta P_{L4,UC} + \Delta P_{gc4}$	(0 x 0) +0.0115 = 0.0115

The steady output of GCs in Area-1 and Area-2 during contract violation is calculated and given in Table 4. It is worthwhile to note that the power output of GC_2 is 0 since A_2 =0.

Retrieval Number: I8711078919/19©BEIESP
DOI: 10.35940/ijitee.I8711.0881019
Journal Website: www.ijitee.org

Published By:
Blue Eyes Intelligence Engineering and Sciences Publication (BEIESP)

Similarly in Area-2, A_3=1 since there is no contract violation ,the GC_3 output remains same as in Case 2, Also A_4 =0 which eventually result in the same power output of 0.0115 puMW.$\Delta P_{L1,UC}$ and $\Delta P_{L2,UC}$ are taken as 0.005 p.u MW and the steady state output of the four Gencos are calculated using Eqn. (9), .as follows:

$\Delta P_{tie12,sch}$=-0.0015p.uMW. The noncontracted load demand of 0.005 p.u MW in Area -1 is met by the generating unit under AGC i.e. GC_1, while the generation of the other Genco i.e. GC_2 in area 1 at steady state is same as previous case.

III. CONTROLLER AND OPTIMIZATION

A. FOPID controller

Fractional calculus is a generalization of the traditional integer-order calculus which encompasses fractional-order integro-differential operators. The transfer function of $PI^{\lambda}D^{\mu}$, the FOPID controller is given by

$$G_c(s) = K_p + \frac{K_i}{s^{\lambda}} + K_d s^{\mu} \tag{10}$$

There are five parameters (K_p, K_i, K_d, λ and μ) that have to be tuned, this improves the flexibility to meet pre-set design demands such as static errors, phase and gain margins, and robustness. The challenge of this work is to create a feasible FOPID controller that achieves the design demands by exhibiting solid efficiency. The main point is to seek acceptable differential operators' approximations λ and s^{μ}. The block diagram of FOPID controller is shown in Fig. 5

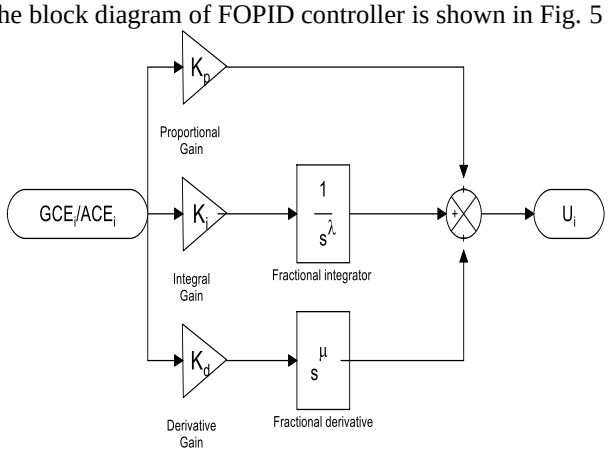

Fig. 5 FOPID controller

B. Objective function

ITAE is used as an objective function for FOPID controller gain tuning through optimization.

$$J = ITAE = \int_0^t |\Delta F_1| + |\Delta F_2| + |\Delta P_{tie}| .t.dt \tag{11}$$

where ΔF_1 and$\Delta F_2$are the system frequency deviation in area-1 and area -2 respectively. ΔP_{tie} is the incremental change in tie-line power and t is the time interval of simulation. The boundaries on controller gains are the constraints. The design problem can, therefore, be formulated as,

Minimize *J*,subjected to

$$K_{PL} \le K_P \le K_{PU} \tag{12a}$$

$$K_{IL} \le K_I \le K_{IU} \tag{12b}$$

$$K_{DL} \le K_D \le K_{DU} \tag{12c}$$

$$\lambda_L \le \lambda \le \lambda_U \tag{12d}$$

$$\mu_L \le \mu \le \mu_U \tag{12e}$$

where *J* is the objective function denoted in (11) and the minimum and maximum bounds for the controller gains and the fractional operators are given in Eqns.12.a -12. e.

C. MFO Algorithm [25]

MFO algorithm exploits moths' navigation behavior during night time. Moths use transverse orientation mechanism to fly at night using the moon. Moths have a unique technique of travelling in a straight line maintaining their respective distance with the moon light as flame. This technique is incorporated in the algorithm taking moths as search agents and the flame as the solution set. The solution set is updated with the position of each moth and the better position is stored. The initial population of moths is randomly generated and the evaluation criterion compares the best moths to that of the best flames, which corresponds to the best optimal values. Flames are often updated by the moths which make sure that the moths never lose best solutions and are retained as flags. The flame matrix, moth matrix, spiral motion of moth is all considered as parameters changing in each iteration. The optimization problem is assumed to be of *d*-dimension with n- decision variables in the search space with desired values. The search space consists a population of *n*-moths as search agents in which each moth has a d-dimensional vector value as the candidate solution to the issue. In d-dimensional space, the moths are flying and their positions are the potential solutions. The following n x d matrix describes the collection of moths and their positions.

$$M = \begin{bmatrix} M_{11} & M_{12} & \cdots & M_{1d} \\ M_{21} & M_{22} & \cdots & M_{2d} \\ \vdots & \vdots & \vdots & \vdots \\ M_{n1} & M_{n2} & \cdots & M_{nd} \end{bmatrix} \tag{13}$$

The vector OM stores the fitness values as:

$$OM = \begin{bmatrix} OM_1 \\ OM_2 \\ \vdots \\ OM_n \end{bmatrix} \tag{14}$$

The flames are represented by the following matrix

Published By:
Blue Eyes Intelligence Engineering
and Sciences Publication (BEIESP)

$$F = \begin{bmatrix} F_{11} & F_{12} & \cdots & F_{1d} \\ F_{21} & F_{22} & \cdots & F_{2d} \\ \vdots & \vdots & \vdots & \vdots \\ F_{n1} & F_{n2} & \cdots & F_{nd} \end{bmatrix} \quad (15)$$

The fitness values of flames are stored in a vector given as:

$$OF = \begin{bmatrix} OF_1 \\ OF_2 \\ \vdots \\ OF_n \end{bmatrix} \quad (16)$$

From mathematical point of view, MFO has three components:

$$MFO = (I, P, T) \quad (17)$$

where I is the function which generates a random population of moths and corresponding fitness values, P is the update function and T is the termination function.
The upper and lower bound decision variables ub and lb are two vectors which are represented as follows:

$$ub = [ub_1, ub_2, \ldots, ub_d] \quad (18)$$

$$lb = [lb_1, lb_2, \ldots, lb_d] \quad (19)$$

The iteration can be initiated once the function I produces the original solution and the function P runs in iterations until the termination is announced by the function T. The update feature, P is the primary component of the MFO moving moths around the search space and updating the flames position. The MFO algorithm flow chart is shown in Fig.6.

D. Implementation

For the proposed system, FOPID controller is applied for the three cases under consideration. MATLAB Simulink 2014, has been used for simulation. Moth Flame Optimization algorithm is used for optimizing the ITAE of the errors ACE and GCE of both the areas. For comparison, the PID controller is also applied for all the three cases. The parameters of the MFO algorithms are number of search agents, which is chosen as 30 and maximum number of iterations is chosen as 100. After several simulations, the limits on the controller gains are selected as, $-10 \le K_P, K_I, K_D \le 10$, $0.5 \le \lambda_i \le 1.5$, $0.5 \le \mu_i \le 1.5$

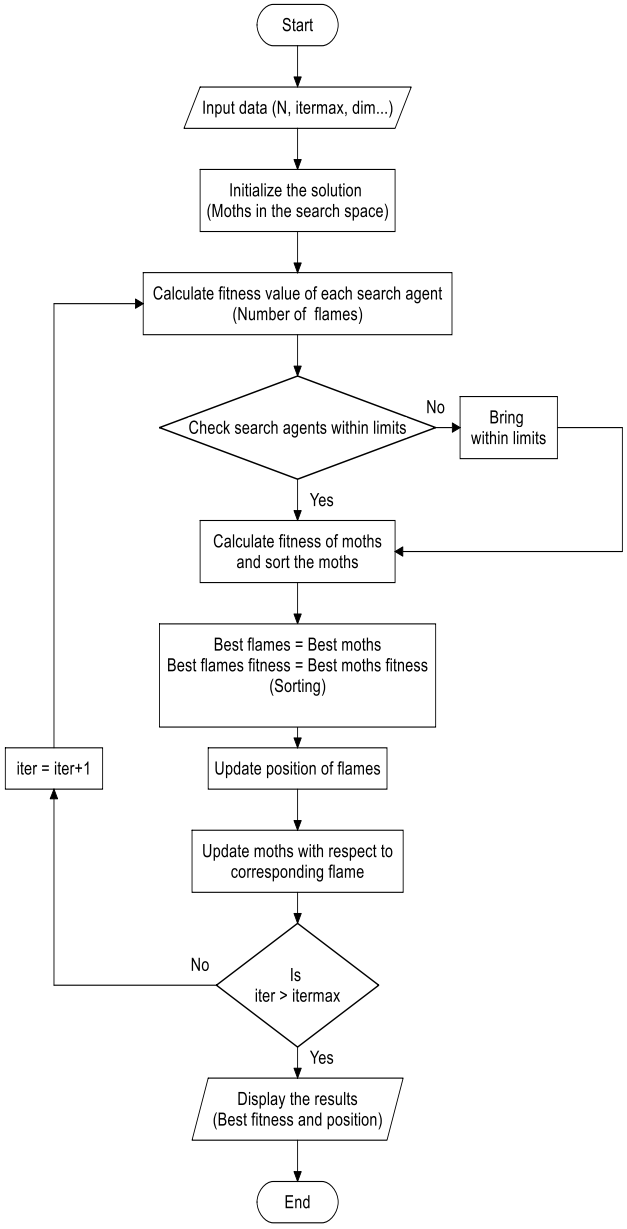

Fig. 6 MFO Optimization flowchart

IV. SIMULATION RESULTS

The objective function, ITAE values obtained using MFO algorithm for the three cases are given in Table 5 and graphically compared in Fig.7 and values. The optimized gains achieved through MFO are depicted in Table 6 for Case 1 and Case 2. The optimized gains for Case 3 are given in Table 7.

Table 5: Comparative performance indexes of different algorithms

	ITAE	
	FOPID	PID
Case1	0.0012	0.0030
Case 2	0.0156	0.0318
Case 3	0.0046	0.0077

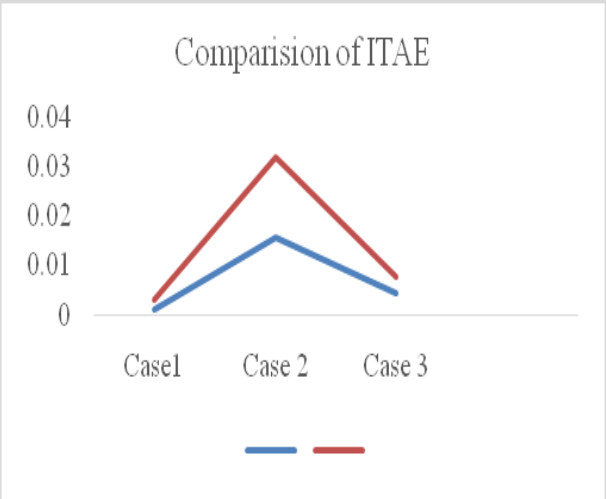

Fig.7 Comparison of ITAE

Table 6: Controller gains tuned by optimization algorithms- Case 1 & Case 2

	Gains	PID	FOPID
Case 1	K_{p1}	2	1.9588
	K_{p2}	2	4.9878
	K_{i1}	1.9040	4.9968
	K_{i2}	1.6529	5
	K_{d1}	0.3250	0.7693
	K_{d2}	0.2699	0.6142
	λ_1	-	0.9988
	λ_2	-	1.0002
	μ_1	-	0.5000
	μ_2	-	0.6515
Case 2	K_{p1}	1.9994	4.9945
	K_{p2}	0.3092	5
	K_{p11}	2	0.001
	K_{p22}	0.2161	0.0136
	K_{i1}	1.9996	5
	K_{i2}	0.0099	4.9973
	K_{i11}	2	-0.8817
	K_{i22}	0.0011	-0.7960
	K_{d1}	0.7010	0.001
	K_{d2}	0.8000	5
	K_{d11}	0.5325	0.0061
	K_{d22}	0.4023	0.001
	λ_1	-	1.4025
	λ_2	-	1.0043
	λ_3	-	1.1390
	λ_4	-	1.5000
	μ_1	-	0.5000
	μ_2	-	0.5000
	μ_3	-	1.4467
	μ_4	-	0.5480

Table 7: Controller gains tuned by optimization algorithms- Case 3

	Case 3	
Gains	FOPID	PID
K_{p1}	5	2
K_{p2}	0.001	0.001
K_{i1}	4.9934	1.7414
K_{i2}	0.3551	0.001
K_{d1}	5	2
K_{d2}	-0.7828	-0.9989
K_{p11}	5	2
K_{p22}	-0.2118	0.0001
K_{i11}	0.0950	0.0011
K_{i22}	0.001	0.0587
K_{d11}	1.5277	1.1746
K_{d22}	0.001	0.001
λ_1	1.0088	-
λ_2	1.0047	-
λ_3	1.0003	-
λ_4	0.6352	-
μ_1	1.4937	-
μ_2	1.0654	-
μ_3	0.5058	-
μ_4	1.4629	-

The quantitative performance comparison of the FOPID and PID controllers are shown in table 8 for Case 1 and Case 2. The performance indices obtained for Case 3 using PID and FOPID are compared and shown in Table 9.

Table 8: Comparison frequency deviation performance indexes

	Area	Performance Index	FOPID	PID	Rajesh [19].
Case 1	Area 1	ST (s)	7.5	8	30
		US (Hz)	-0.0064	-0.0075	-0.0800
		OS (Hz)	0.0018	0.003	0.0400
	Area 2	ST (s)	7.8	9	30
		US (Hz)	-0.0033	-0.0048	-0.0800
		OS (Hz)	0.0016	0.0031	0.04000
Case 2	Area 1	ST (s)	7	10	45
		US (Hz)	-0.0058	-0.008	-0.08
		OS (Hz)	0.0023	0.005	0.06
	Area 2	ST (s)	10	15	45
		US (Hz)	-0.003	-0.005	-0.08
		OS (Hz)	0.0028	0.006	0.06

Retrieval Number: I8711078919/19©BEIESP
DOI: 10.35940/ijitee.I8711.0881019
Journal Website: www.ijitee.org

Published By:
Blue Eyes Intelligence Engineering and Sciences Publication (BEIESP)

Table 9: Comparison frequency deviation performance indices Case 3

	Area	Performance Index	FOPID	PID	Rajesh [19].
Case 3	Area 1	ST (s)	7	13	55
		US (Hz)	-0.017	-0.0143	-0.15
		OS(Hz)	0.004	0.003	0.12
	Area 2	ST (s)	7	17	55
		US (Hz)	-0.0065	-0.0037	-0.15
		OS (Hz)	0.0008	0.0035	0.12

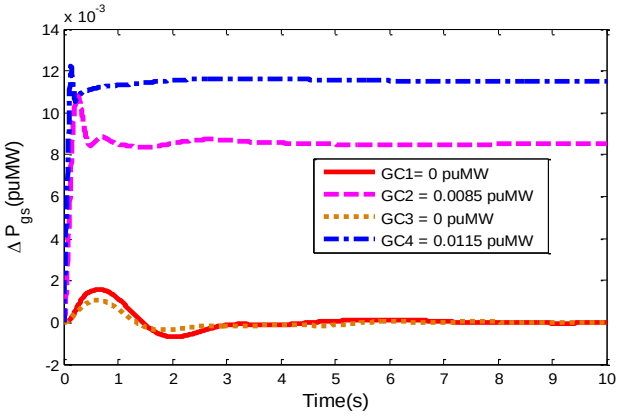

Fig.11 Case1: Power outputs of GCS at steady state

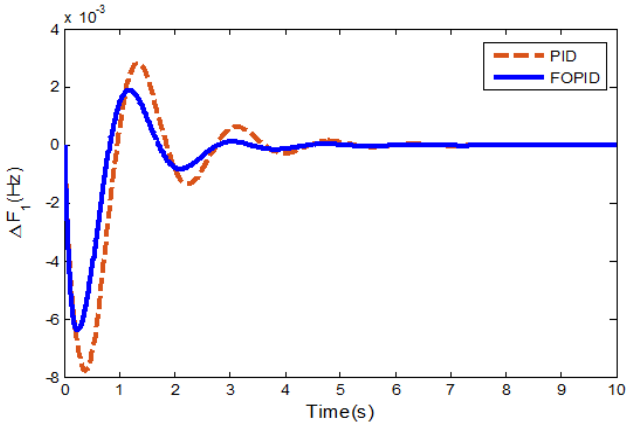

Fig. 8 Case1: Frequency deviation in Area-1

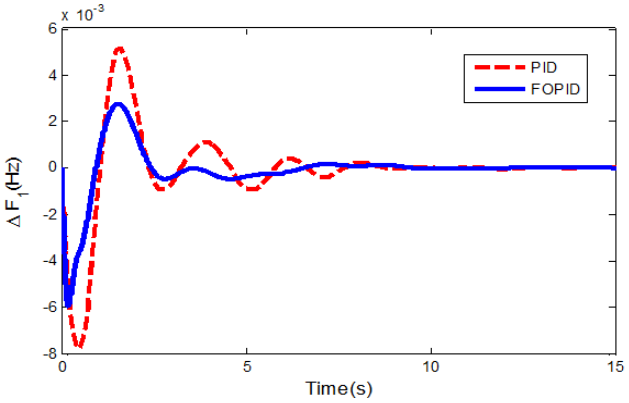

Fig.12 Case2: Frequency deviation in Area-1

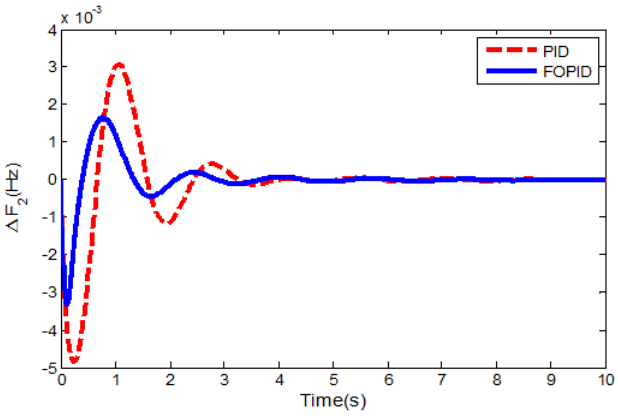

Fig. 9 Case1: Frequency deviation in Area-2

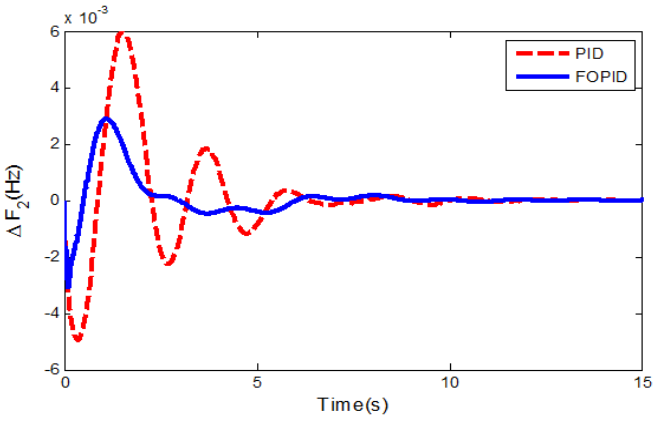

Fig.13: Case2: Frequency deviation in Area-2

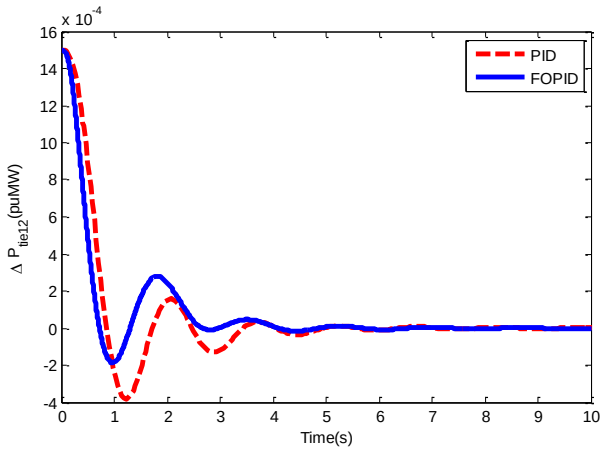

Fig.10 Case1: Tie-line power deviation between Area-1 and Area-2

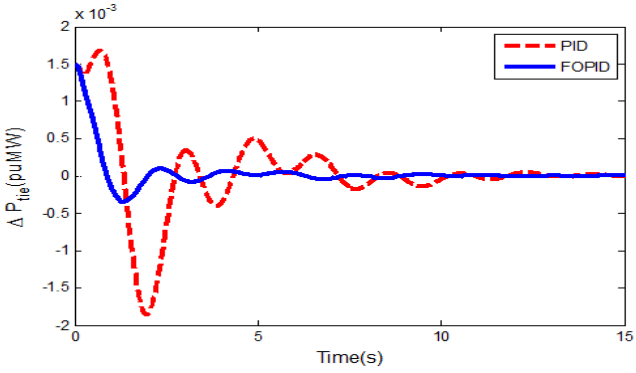

Fig.14 Case 2: Tie-line power deviation between Area-1 and Area-2

Retrieval Number: I8711078919/19©BEIESP
DOI: 10.35940/ijitee.I8711.0881019
Journal Website: www.ijitee.org

Published By:
Blue Eyes Intelligence Engineering and Sciences Publication (BEIESP)

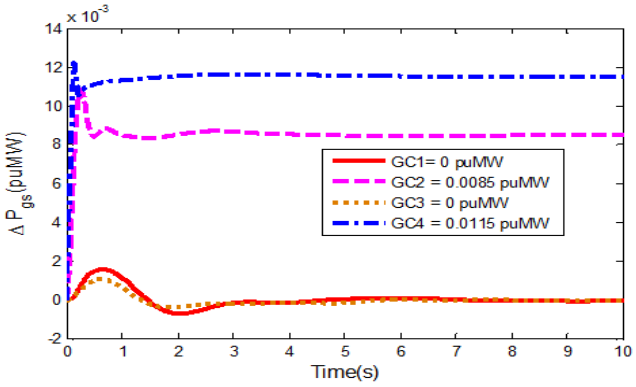

Fig.15 Case2: Power outputs of GCS at steady state

The output responses obtained using FOPID and PID controllers for Case 1 are shown from Fig.8 to Fig.11. The output responses obtained using FOPID and PID controllers for Case 2are shown from Fig.12 to Fig.15

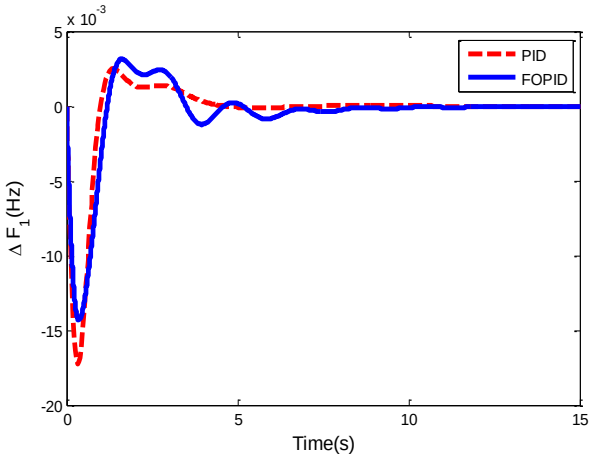

Fig.16 Case 3: Frequency deviation in Area-1

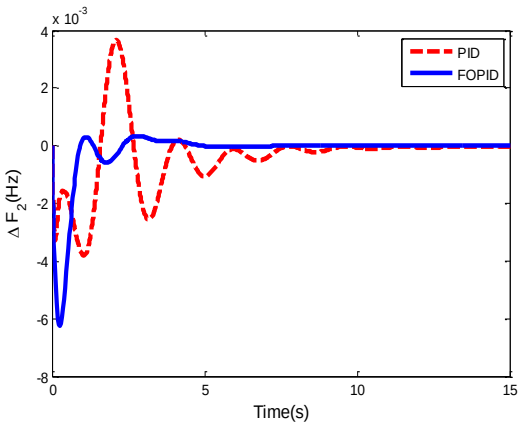

Fig.17 Case 3: Frequency deviation in Area-2

Area-1 and Area-2 frequency deviations obtained using the optimized PID and FOPID gains for Case 3 are shown in Fig.16 and Fig.17. The tie-line power deviation and the Genco outputs are shown in Fig.18 and Fig.19 respectively. The Genco outputs for Case 3 are calculated and given in Table 10.

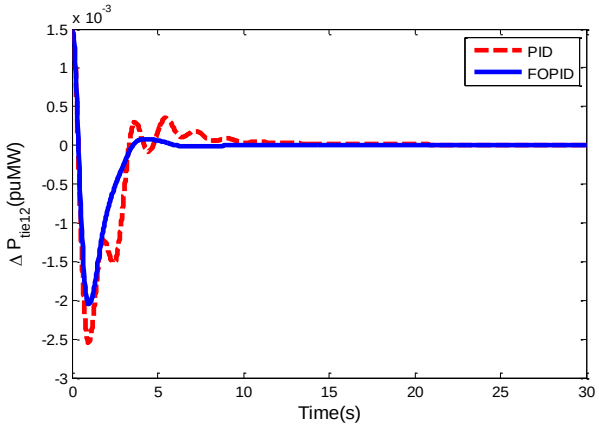

Fig. 18 Case 3 Tie-line power deviation between Area-1 and Area-2

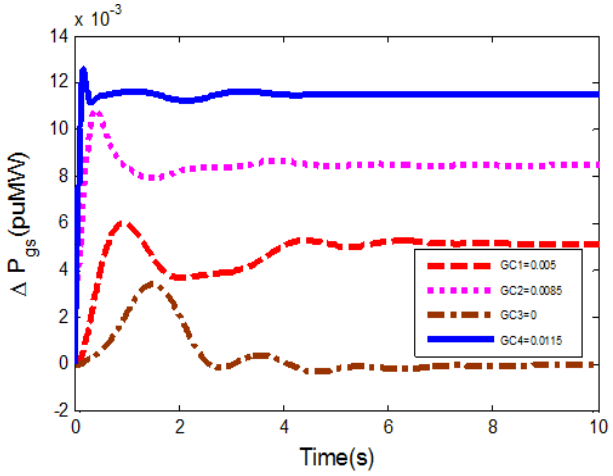

Fig. 19 Case3: Power outputs of GCS at steady state

Table 10: GENCOs output power -Case 3

	Area-1		Area-2			Total (puMW)
	DC_1	DC_2	DC_3	DC_4	Noncontracted demand	
GC_1	0	0	0	0	0.005	0.005
GC_2	0.00125	0.0005	0.00375	0.003	-	0.0085
GC_3	0	0	0	0	-	0
GC_4	0.00375	0.0045	0.00125	0.002	-	0.0115

V. CONCLUSION

In this work, an effort has been made to analyze the practicability of affording optimized frequency control as an ancillary service using FOPID controller optimized by MFO algorithm in a competitive power market.

The performance of FOPID controller has been compared with that of the classical PID controller in the two area inter connected non-reheat thermal power system. Three different cases under bilateral contract scenario have been analyzed. The gains of the AGC and Load following FOPID controllers are optimized by the MFO algorithm using ITAE of ACE and GCE as objective function and it has been found that FOPID is effective in bringing the frequency deviation and tie line power deviations to zero. In all the three cases, the contracted amount of power demanded by the DCs has been supplied by the corresponding GCs. On comparison of the results with that of [19], the effectiveness of FOPID controller is established.

REFERENCES

1. P. Kundur, J. Paserba, V. Ajjarapu, G. Andersson, A. Bose, C. Canizares, and T. Van Cutsem, "Definition and classification of power system stability," *IEEE transactions on Power Systems*, vol. 19, no. 2, 2004, pp. 1387-1401.
2. R. Christie, D. and A. Bose, "Load frequency control issues in power system operations after deregulation," *IEEE Transactions on Power systems*, vol. 11, no. 3, 1996, pp. 1191-1200.
3. E. Hirst, and B. Kirby, "Separating and measuring the regulation and load-following ancillary services," *Utilities Policy*, vol. 8, no. 2, 1999, 75-81.
4. V. Donde, M. A. Pai, and I. A. Hiskens, "Simulation and optimization in an AGC system after deregulation," *IEEE transactions on power systems*, vol. 16, no. 3, 2001, pp. 481-489.
5. E. Nobile, A. Bose, and K. Tomsovic, "Feasibility of a bilateral market for load following," *IEEE Transactions on Power systems*, vol. 16, no. 4, 2001, pp. 782-787.
6. B. Tyagi, and S. C. Srivastava, "A decentralized automatic generation control scheme for competitive electricity markets," *IEEE transactions on power systems*, vol. 21, no. 1, 2006, pp. 312-320.
7. P. Bhatt, R. Roy, and S. P. Ghoshal, "Optimized multi area AGC simulation in restructured power systems," *International journal of electrical power & energy systems*, vol. 32, no. 4, 2010, pp. 311-322.
8. F. Liu, Y. H. Song, J. Ma, S. Mei, and Q. Lu, "Optimal load-frequency control in restructured power systems," IEE *Proceedings-Generation, Transmission and Distribution*, vol. 150, no. 1, 2003, pp. 87-95.
9. I. A. Chidambaram, and B. Paramasivam, "Optimized load-frequency simulation in restructured power system with redox flow batteries and interline power flow controller," *International Journal of Electrical Power & Energy Systems*, vol. 50, 2013, pp. 9-24.
10. P. Dahiya, V. Sharma, and R. Naresh, "Automatic generation control using disrupted oppositional based gravitational search algorithm optimised sliding mode controller under deregulated environment," *IET Generation, Transmission & Distribution*, vol. 10, no. 16, 2016, pp. 3995-4005.
11. G. Sharma, K. R. Niazi, and R. C. Bansal, "Adaptive fuzzy critic based control design for AGC of power system connected via AC/DC tie-lines," *IET Generation, Transmission & Distribution*, vol. 11, no. 2, 2017, pp. 560-569.
12. S. H. Hosseini, and A. H. Etemadi, "Adaptive neuro-fuzzy inference system based automatic generation control," *Electric Power Systems Research*, vol. 78, no. 7, 2008, pp.1230-1239. https://doi.org/10.1016/j.epsr.2007.10.007
13. H. Shayeghi, H. A. Shayanfar, and O. P. Malik, "Robust decentralized neural networks based LFC in a deregulated power system," *Electric Power Systems Research*, vol. 77, no. 3-4, 2007, pp. 241-251.
14. L.C Saikia, S. Mishra, N. Sinha, and J. Nanda, "Automatic generation control of a multi area hydrothermal system using reinforced learning neural network controller," *International Journal of Electrical Power & Energy Systems*, vol. 33, no. 4, 2011, pp. 1101-1108.
15. H. Shayeghi, H. A. Shayanfar, and A. Jalili, "Multi-stage fuzzy PID power system automatic generation controller in deregulated environments," *Energy Conversion and management*, vol. 47, no. 18-19, 2006, pp. 2829-2845.
16. T. S. Gorripotu, H. Samalla, C. J. M. Rao, A. T. Azar, and D. Pelusi, "TLBO Algorithm Optimized Fractional-Order PID Controller for AGC of Interconnected Power System," *In Soft Computing in Data Analytics*, 2019, (pp. 847-855). Springer, Singapore.
17. Y. Arya, "AGC of restructured multi-area multi-source hydrothermal power systems incorporating energy storage units via optimal fractional-order fuzzy PID controller," *Neural Computing and Applications*, vol. 31, no. 3, 2019, pp. 851-872.
18. Z. X. Tang, Y. S. Lim, S. Morris, J. L. Yi, P. F. Lyons, and P. C. Taylor, "A comprehensive work package for energy storage systems as a means of frequency regulation with increased penetration of photovoltaic systems," *International Journal of Electrical Power & Energy Systems*, vol. 110, 2019, pp. 197-207.
19. R. J. Abraham, D. Das, and A. Patra, "Load following in a bilateral market with local controllers," *International Journal of Electrical Power & Energy Systems*, vol. 33, no. 10, 2011, pp. 1648-1657.
20. D. H. Wolpert, and W. G. Macready, "No free lunch theorems for optimization," *IEEE transactions on evolutionary computation*, vol. 1, no. 1, 1997, pp. 67-82.
21. K. B. Oldham, and J. Spanier, "The fractional calculus theory and applications of differentiation and integration to arbitrary order," *Academic Press*, New York, 1974, PP. 111.
22. K. S. Miller, and B. Ross, "An Introduction to the Fractional Calculus and Fractional Differential Equation," *Wiley*, New York, 1993.
23. I. Podlubny, "Fractional-order systems and PI/sup/spl lambda//D/sup/spl mu//-controllers," *IEEE Transactions on automatic control*, vol. 44, no. 1, 1999, pp. 208-214.
24. R. El-Khazali, W. Ahmad, and Y. Al-Assaf, "Sliding mode control of generalized fractional chaotic systems," *International Journal of Bifurcation and Chaos*, vol. 16, no. 10, 2006, pp. 3113-3125.
25. S.Mirjalili, "Moth-flame optimization algorithm: A novel nature-inspired heuristic paradigm," *Knowledge-Based Systems*, vol. 89, 2015, pp. 228-249.
26. S. Reddy, L. K. Panwar, B. K. Panigrahi, and R. Kumar, "Solution to unit commitment in power system operation planning using binary coded modified moth flame optimization algorithm (BMMFOA): a flame selection based computational technique," *Journal of Computational Science*, vol. 25, 2018, pp. 298-317.
27. B. V. S. Acharyulu, B. Mohanty, and P. K. Hota, "Comparative performance analysis of PID controller with filter for automatic generation control with moth-flame optimization algorithm," *In Applications of Artificial Intelligence Techniques in Engineering*, 2019, (pp. 509-518). Springer, Singapore. https://doi.org/10.1007/978-981-13-1819-1_48
28. A. K. Barisal, AND l. K. Lal, "Application of moth flame optimization algorithm for AGC of multi-area interconnected power systems," *International Journal of Energy Optimization and Engineering (IJEOE)*, vol.7, no. 1, 2018, pp. 22-49.
29. M. A. Taher, S. Kamel, F. Jurado, and M. Ebeed, "An improved moth-flame optimization algorithm for solving optimal power flow problem," *InternationalTransactions on Electrical Energy Systems*, vol. 29, no. 3, 2019, pp. e2743.

Appendix I Nomenclature

GC	Genco
DC	Disco
ΔP_L	Change in Load Demand
K_p	Gain of the power system
T_p	Time constant of the system (s)
T_t	Time constant of the turbine (s)
T_g	Time constant of the Governor (s)
T_{12}	Time constant of the tie-line (s)
R	Speed regulation (Hz/p.u.MW)
ΔF	Frequency deviation (Hz)
ΔP_{tie12}	Deviation in Tie line power exchange between Area -1 and Area-2
$\Delta P_{L1,UC}$	Un-contracted load demand
A_1, A_2	ACE participation factors of GCs 1 & 2 in area-1
A_3, A_4	ACE participation factors of GCs 3 &4 in area-2
B_1, B_2	Frequency bias factors

Retrieval Number: I8711078919/19©BEIESP
DOI: 10.35940/ijitee.I8711.0881019
Journal Website: www.ijitee.org

Published By:
Blue Eyes Intelligence Engineering and Sciences Publication (BEIESP)

K_{p1},K_{i1},$K_{d1}\lambda_1$,μ_1	Gains of Load following controller for GC_2
K_{p2},K_{i2},$K_{d2}\lambda_2$,μ_2	Gains of Load following controller for GC_4
K_{p11},K_{i11}, $K_{d11}\lambda_3$,μ_3	Gains of AGC controller in area-1
K_{p22},K_{i22}, K_{d22} ,λ_4,μ_4	Gains of AGC controller in area-2

Appendix IINominal Values Of System Parameters

K_{pi}= 120
T_{gi}=0.08 s
T_{ti}=0.3 s
T_{pi} = 20 s
R_i=2.4 Hz/pu.MW
B_i= 0.425
T_{ij} = 0.0866

AUTHORS PROFILE

S. Jennathu Beevi received the B.E. degree fromthe Department of Electrical and Electronics Engineering, University of Madras , India, 1998. She obtained her M.E degree in Power System Engineering from B.S.A. Crescent Engineering College. She was awarded the Silver Medalfor securing the second rank in M.E. Power System by Anna Universityin the year 2004.She is working as Assistant Professor (Senior Grade) in the department of Electrical and Electronics Engineering, B.S.Abdur RahmanInstitute of Science and Technology, Chennai. She is currently pursuing her Ph.D at B.S.Abdur RahmanInstitute of Science and Technology in the area of Automatic Generation Control in Deregulated Environment. She has been teaching for the past 16 years. Her research interests are in the field of optimization in deregulated power system, power system control and soft computing.

Dr. R. Jayashree secured her B.E degree in Electrical and Electronics Engineering in the year 1990 with a First class from Thiagarajar College of Engineering, Madurai. She secured her M.E degree in Power System Engineering with first class with distinction at Anna University, Chennai in the year 1992. She secured first rank in M.E degree. She secured her Ph.D degree in Electrical Engineering at Anna University, Chennai in the year 2008. She is currently currently working as Professor at B.S.Abdur Rahman Institute of Science and Technology.She has been teaching for the past 23 years. She is a member of IEEE. She has to her credit about 55 papers published /presented in the National and International journals/conferences. Her areas of interest include ATC and congestion management, Load Frequency Control, Reactive power allocation and pricing etc.